RESEARCH

HPLC–HR-ESI–MS/MS identification of fluorescent dyes and optical brighteners and their degradation products in daylight fluorescent paints

Lukas Reiß[1,2*] , Susanne Machill[1] , Tilo Lübken[3] and Christoph Herm[2]

Abstract

Daylight fluorescent paints are luminous colors that are increasingly used in contemporary art. The pigments consist of a synthetic resin in which fluorescent dyes and optical brighteners are embedded. In the recent years, several research articles have been published on the composition of daylight fluorescent pigments. Despite the growing research on the aging behavior of daylight fluorescent paints, little is known to date about the chemical processes involved in aging. In the research presented here, we used dialysis to separate the colorants from the resin. HPLC–HR-ESI–MS/MS was used to extend the elucidation of the dye composition. A variety of rhodamines and coumarins, an aminonaphthalimide dye and another optical brightener were determined. NMR was used to elucidate the structure of an additional hemicyanine dye not listed in the Colour Index. Furthermore, reference substances were artificially aged under visible light and UV radiation and the degradation products were analyzed accordingly. N-deethylation, hydroxylation and higher oxidation processes were found to be the main degradation pathways for all colorants. For most dyes and optical brighteners, there was no difference between aging under visible light and aging under UV radiation. When the results were checked on samples of aged paint mock-ups, it was found that only a few of the degradation products can still be detected in the case of very advanced aging even with the smallest sample quantities.

Keywords Daylight fluorescent paints, HPLC–HR-MS/MS, Artificial aging, Degradation products

Introduction

In recent years, research in the composition of daylight fluorescent pigments (DFPs) for conservational purposes has increased rapidly. Since their development in the middle of the last century, these luminous pigments have attracted great interest from well-known artists [1].

*Correspondence:
Lukas Reiß
lukas.reiss@tu-dresden.de
[1] Chair of Bioanalytical Chemistry, Technische Universität Dresden, Bergstraße 66, 01069 Dresden, Germany
[2] Laboratory of Archaeometry, Dresden University of Fine Arts, Güntzstraße 34, 01307 Dresden, Germany
[3] Chair of Organic Chemistry I, Technische Universität Dresden, Bergstraße 66, 01069 Dresden, Germany

The chemical composition of DFPs, which on the one hand leads to the eye-catching appearance, has on the other hand the disadvantage of a significantly lower light fastness compared to conventional pigments [2]. DFPs consist of a synthetic polymer resin in which mainly fluorescent dyes, but also non-fluorescent dyes and pigments as well as optical brighteners and other additives are embedded. The resin serves to increase the light fastness of the dyes as well as to dilute the dyes, since—depending on the dye—concentration quenching of luminescence already occurs at concentrations above 1% [3].

The resin usually consists of a toluenesulfonamide component and an amine component, which is typically melamine, but other triazines such as benzoguanamine are also used. A melamine toluenesulfonamide

Reiß *et al. Heritage Science*   (2023) 11:146

Page 2 of 17

formaldehyde resin (MSF resin) is used in the DFPs from Kremer Pigmente, which were analyzed in the present study [4]. The resin itself has excellent light stability. For special requirements on pigment properties such as high heat resistance, DFPs with resins based on polyesters, polyamides and polyurethane are on the market, too [2]. The dyes, pigments and additives are added to this resin during polymerization. The additives comprise organic UV absorbers such as oxybenzone and inorganic UV absorbers such as TiO_2 and ZnO_2 as well as alkanes, alkenes and alcohols [4]. An approach to identify resin components and to differentiate between products from different manufacturers based on the resin components and was recently published by Álvarez-Martín et al. [4].

The identification of the dyes has been widely approached in the literature using Raman spectroscopy [5–7] or—after separation via thin-layer chromatography (TLC)—with surface-enhanced Raman spectroscopy (SERS) [6, 7]. Besides the advantage of easy use and interpretation via spectral databases as well as the possibility of combination with separation techniques such as TLC, Raman spectroscopy also brings some disadvantages:

- When analyzing the pigments without prior separation, often only the main dyes in the pigments can be detected in addition to the resin. Especially for the green and blue DFPs of different manufacturers, the Raman spectra often revealed only Pigment Green 7 (PG7) and Pigment Blue 15:3 (PB15:3) which dominated the spectra [5, 6]. (Dyes and pigments are designated with Colour Index Generic Names in this study.)
- Dyes with the same molecular framework, such as differently substituted rhodamines or coumarins, often show very similar Raman spectra. In many cases, these derivatives cannot be separated sufficiently via TLC, neither. Depending on the availability of reference substances and their spectra, this often leads to either multiple interpretations or misinterpretation of the spectra. Especially for SERS, databases often are not developed enough and not all substances can be identified on TLC plates with SERS.

Schmidtke Sobeck et al. then used a more comprehensive method consisting of separation by high-performance liquid chromatography with subsequent detection by a diode array detector and a mass spectrometer (HPLC–DAD–MS), with which even very similar substances could be separated and distinguished [8]. This study showed that the rhodamines, which were previously identified as Rhodamine 6G and Rhodamine B in the Raman studies because they are the most common

rhodamines and available in most of the reference databases, are actually mixtures of various esters of these two dyes, as well as Sulforhodamine B. Furthermore, it turned out that the yellow dye determined by Campanella et al. by means of SERS as Solvent Yellow 160:1 is in fact Solvent Yellow 172, which both have the same benzoxazolylcoumarin framework but differ in substituents [7, 8]. The study by Schmidtke Sobeck et al. examined the DFP series from Kremer Pigmente, which were also examined in the present study, and thus serves as an excellent comparative study.

Some studies addressed the phenomenological behavior of paint mock-ups during light aging [9–13]. The main findings of these studies were that light aging of daylight fluorescent paints results in color fading and a blue shift in fluorescence. TLC [12] and Raman spectroscopy [13] confirmed the degradation of individual dyes during aging.

Despite these numerous studies to determine the dye and resin composition of DFPs and the photographic and spectroscopic documentation of the aging process, little is known at present about the reactions on the molecular level during photochemical degradation of daylight fluorescent dyes and optical brighteners. Thus, the aim of this study is to extend the elucidation of the degradation mechanisms of dyes and optical brighteners in DFPs. The possibility of identifying degradation products in real paint samples should facilitate the determination of DFPs in works of art, even when they are not visible anymore.

Due to the extensive use of triarylmethane dyes such as rhodamines in the textile, food and cosmetics industries [14], they contribute significantly to environmental pollution [15]. Therefore, comprehensive research has already been carried out on the catalysis-accelerated degradation of Rhodamine B and its reactions pathways in aqueous solution [16–18]. These studies showed that Rhodamine B degradation occurs via two simultaneous mechanisms: N-deethylation and the cleavage of the chromophore system by photo-generated active oxygen species.

Coumarin dyes tend to have a higher light fastness than rhodamines [19]. Winters et al. also determined the degradation products formed from the laser dye 7-diethylamino-4-methylcoumarin [20], which is also used in DFPs as optical brightener [8]. Similar to rhodamines, N-deethylation and additionally the oxidation of the methyl substituent were detected. Jones and Bergmark demonstrated the reduction of the lactone moiety and confirmed that self-quenching occurs in the degradation of coumarins at high concentrations [21]. Sokołowska et al. showed that coumarin dyes substituted with different heterocycles have partially the same degradation products. Therefore, substituent abstraction also occurs as a degradation reaction [22].

Reiß *et al. Heritage Science*   (2023) 11:146

Page 3 of 17

In the present study, the degradation products of the dyes and optical brighteners contained in the DFPs from Kremer Pigmente were determined by high-performance liquid chromatography coupled with high-resolution tandem mass spectrometry (HPLC–HR-MS/MS). For this purpose, reference substances were artificially aged using visible light (VIS aging) and UV radiation (UV aging), respectively. The aging behavior of the dyes depends strongly on the matrix. For example, Reisfeld et al. demonstrated increased stability of Rhodamine 6G in a polymer matrix [23], as is the case with DFPs. Therefore, an attempt was also made to detect the degradation products in samples of aged paint mock-ups containing DFPs from a previous study [13].

Materials and methods
Materials
The dyes and optical brighteners were identified in the DFPs from Kremer Pigmente: White (#56000), Blue (#56050), Green (#56100), Lemon Yellow (#56150), Golden Orange (#56200), Orange (#56250), Brick Red (#56300), Flame Red (#56350), Cyclamen Red (#56400) and Violet (#56450).

The identification of the degradation products was carried out on the following substances that were found to be constituent of the DFPs from Kremer Pigmente: Sulforhodamine B (SRB; #082P1700), Basic Violet 11 (BV11; #134P0401), Basic Violet 11:1 (BV11:1; #124P0400), Basic Yellow 40 (BY40; #047P0402), Solvent Yellow 44 (SY44; #073P0407) and Solvent Yellow 172 (SY172; #045P0408),

kindly provided by Neelikon Food Dyes & Chemicals, Ltd.; Rhodamine 6G (Rh6G; #0749.1), Rhodamine 575 (Rh575; #7310.2) and Rhodamine B (RhB; #T130.1) from Carl Roth; Fluorescent Brightener 184 (FB184; #A14928) from Alfa Aesar; Basic Red 1:1 (BR1:1) from WinChem Industrial Co., Ltd.; 7-Diethylamino-4-methylcoumarin (Fluorescent Brightener 61; FB61; #D87759) from Sigma-Aldrich. The structures are given in Fig. 1. Additional information (synonyms, identifiers, exact mass, MS/MS fragments) are given in Additional file 1: Table S1.

Samples of the following paint mock-ups were analyzed: Blue (after 16.3 kWh/m^2 UV aging); Lemon Yellow, Brick Red and Violet (after 360 Mlxh VIS aging) [13].

Resin removal from the pigments and paint samples via dialysis
For HPLC, it is necessary to remove the resin from the dyes and optical brighteners. In the literature, this was approached by solid phase extraction of dissolved pigments (from DayGlo Color Corp. [24]). However, the same experiments for the pigments from Kremer Pigmente showed that at least one violet dye eluted only at a methanol concentration at which the resin was co-eluted. Therefore, dialysis was chosen as the purification method instead: Approximately 0.04 g of the pigment is suspended in 1 ml acetone in a 1.5 ml microcentrifuge tube and centrifuged at 6000 rpm for 15 min. The White pigment showed a significantly higher solubility than the other pigments because its resin is not a thermoset but a thermoplastic [4]. For concentration, the supernatant
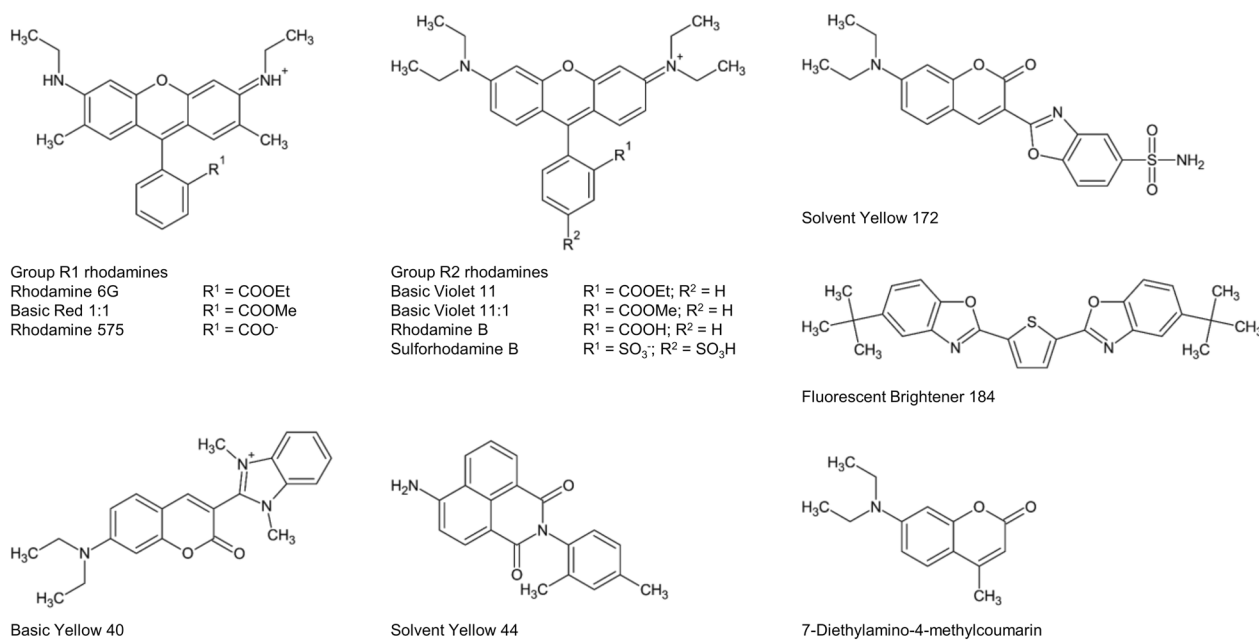

Group R1 rhodamines
Rhodamine 6G   R^1 = COOEt
Basic Red 1:1   R^1 = COOMe
Rhodamine 575   R^1 = COO$^-$

Group R2 rhodamines
Basic Violet 11   R^1 = COOEt; R^2 = H
Basic Violet 11:1   R^1 = COOMe; R^2 = H
Rhodamine B   R^1 = COOH; R^2 = H
Sulforhodamine B   R^1 = SO$_3^-$; R^2 = SO$_3$H

Solvent Yellow 172

Fluorescent Brightener 184

Basic Yellow 40

Solvent Yellow 44

7-Diethylamino-4-methylcoumarin

Fig. 1 Structures of the dyes and optical brighteners used as reference materials. Counter ions for the cationic dyes are not shown

Reiß *et al. Heritage Science*   (2023) 11:146

Page 4 of 17

solution is transferred to a new tube, evaporated using a nitrogen stream, and then re-dissolved in 0.3 ml acetone. Dialysis was performed in a SLIDE-A-Lyzer Mini Dialysis Device with 2 K MWCO membrane (#69580) from ThermoFisher. GC Ultra Grade acetone (Carl Roth #KK40.1) was used. The sample is transferred to a Mini Dialysis Device, which is then sealed and placed on a microcentrifuge tube filled with 1 ml acetone. The tube is then placed on a shaker plate for 2 h. The Mini Dialysis Device is removed and 1 ml of the sample in the outer tube is transferred to an HPLC vial.

The authors recommend not to inject the acetone extract directly into the HPLC, but to use dialysis or at least syringe filtration beforehand. Acetone extracts could not be evaporated and re-dissolved in ethanol, indicating the presence of the resin, which could lead to column clogging. The dialyzed samples could be evaporated and re-dissolved in ethanol (which has a lower solubility of the resin compared to acetone), signaling the separation from the resin.

For the dialysis of the samples taken from the mockups, 0.3 ml of acetone was first added to a sample in a 1.5 ml microcentrifuge tube. The tube was sealed and stored in the dark for 1 week to dissolve the acrylate binder. Dialysis was performed as described above. The solution in the outer tube was evaporated using a nitrogen stream. The residue was taken up in 0.2 ml acetone and transferred to a micro-insert HPLC vial, where it was again evaporated to about half in order to concentrate the sample.

Accelerated light aging

1 mg of each reference dye and optical brightener was dissolved in 5 ml ethanol. For each colorant, 0.1 ml of the solution was added to five HPLC vials. The ethanol was then evaporated at ambient conditions so that a thin film of the dye was deposited on the glass wall of the vials. One of the vials was kept in the dark as reference, two of the vials were exposed to VIS aging and two of the vials were exposed to UV aging. The UV cutoff wavelength of the vials used for the aging experiments was 350 nm.

VIS and UV aging of the reference dyes and optical brighteners were performed in an in-house constructed exposure chamber in which the light sources were mounted on exchangeable lids. The lamps used for VIS aging show a sharp emission band around 458 nm and an emission plateau from 540 to 600 nm. The LEDs used for UV aging show a sharp emission band from 360 to 400 nm with a maximum at 370 nm (precise details and lamp/LED spectra are given in the literature [13]). The emission of the UV LEDs was thus outside the UV cutoff range of the vials used.

For aging, the vials were positioned centrally in the exposure chamber, and the position was swapped regularly. VIS aging was performed for 10 and 30 days, corresponding to an exposure of 20 Mlxh and 62 Mlxh. UV aging was performed for 10 and 30 days, corresponding to a radiant exposure of 15.1 MJ/m^2 and 25.9 MJ/m^2. After aging, the degradation products were dissolved in 1 ml ethanol.

Photography

The solutions of the unaged substances in ethanol, a 1:20 dilution of these, and the aged samples were photographed. Visible light photography (DL photography) was performed with a DSLR camera Nikon D500 and a daylight flash system Elinchrom Digital 2400 RX with one Digital See Flash Head and Softbox. For UV-induced visible fluorescence photography (UVF photography), a Hönle UVAHAND 250 UV lamp was used to excite the colorant solutions and the camera lens was fitted with a Lee Filters 2C UV cut filter.

HPLC–HR-MS/MS

HPLC–HR-MS/MS studies were performed on a 1260 Infinity HPLC system coupled with a 6538 UHD Accurate-Mass quadrupole time-of-flight (Q-TOF) MS with ESI from Agilent Technologies. Separation of the dyes and optical brighteners in the HPLC was performed using a ZORBAX Rapid Resolution HT Extend-C18 2.1×50 mm column with a particle size of 1.8 μm from Agilent Technologies.

HPLC–MS grade water (#10777404) from Fisher Chemical™ and LC–MS grade acetonitrile (ACN; #2697) from Chemsolute® with 0.1% LC–MS grade formic acid (#84865.260) from VWR Chemicals were used as eluents. The gradient from water to ACN used by Hinde [12] was adjusted to elute FB184: 5%–20% ACN (0–5 min), 20%–100% ACN (5–45 min) and 100% ACN (45–50 min). The flow rate was 0.2 ml/min, the column temperature was 25 ℃. 2 μl of the sample were injected for the analysis of the pigments and 10 μl for the analysis of the samples taken from the aged colorants and aged paint samples.

ESI-HR-MS was performed using positive ionization mode with the following settings: N_2 temperature 350 ℃, drying gas 10 l/min, nebulizer 50 psig, ESI VCap 4000 V, fragmentor 100 V, skimmer 45 V, Oct 1 RF Vpp 750 V. Mass spectra were measured in the range 100–1000 m/z. HR-MS/MS was done by fragmenting the (quasi)-molecular ions with N_2 collision gas with 20 eV for smaller molecules (e. g. FB61) to 50 eV for larger molecules (e. g. SRB).

For the identification of the dyes and optical brighteners in the DFPs, the dialyzed samples were analyzed with HPLC–HR-MS/MS. Based on the molecular formula

Reiß et al. Heritage Science   (2023) 11:146

Page 5 of 17

determined, probable dyes were searched in the literature [2, 25, 26]. Subsequently, HPLC–HR-MS/MS of standard solutions of reference substances was used to confirm the assumptions.

For the identification of the degradation products of the reference dyes, the aged dye samples were analyzed with HPLC–HR-MS. HR-MS/MS was performed on several of the peaks.

For the identification of the degradation products in the samples taken from the aged paint mock-ups, the dialyzed samples of the paints were analyzed with HPLC–HR-MS. The degradation products could only be identified based on retention time and exact mass, not by MS/MS, due to very low signal intensity.

NMR spectroscopy

The structure of one dye in the Violet DFP which was not identified by HPLC–HR-MS/MS was elucidated by nuclear magnetic resonance spectroscopy (NMR). For purification, 1 g of the DFP was extracted ten times with 10 ml ethanol for 2 h. After centrifugation, the supernatant solutions were evaporated at 65 °C using a nitrogen stream and then combined. 50.8 mg of the extraction product were fractionated by column chromatography using silica gel 60 (0.063–0.200 mm) as stationary phase and 95% dichloromethane/5% methanol as mobile phase. Deep violet fractions were combined and evaporated under reduced pressure to give 4.1 mg of pure substance.

NMR data were recorded at ambient temperatures on a Bruker Avance III 600 spectrometer operating at 600.2 MHz for ^{1}H, 150.9 MHz for ^{13}C and 60.8 MHz for ^{15}N. Chemical shifts δ are given in ppm relative to TMS (^{1}H and ^{13}C) or CH_3NO_2 (^{15}N). The solvent signals were used as reference for ^{1}H and ^{13}C (^{1}H: δ_H 3.310 ppm residual CHD_2OD, ^{13}C: δ_C 49.00 ppm CD_3OD). For ^{15}N (Ξ = 0.10136767) universal calibration was used [27].

Coupling constants are given in Hz and were determined assuming first-order spin–spin coupling. Nitrogen chemical shifts were taken from ^{1}H/^{15}N-HMBC experiment.

Results

Dyes and optical brighteners in the DFPs from Kremer Pigmente

The semi-quantitative data presented in Table 1 are based on the peak areas in the HPLC–MS chromatograms and on the spot sizes on TLC plates (Additional file 1: Fig. S1, method not discussed further in this study). The results of the HPLC–MS and TLC were mainly consistent, although the dyes present only in trace amounts were not detectable on the TLC plates. SRB showed comparatively low peak areas in the HPLC–MS chromatograms but large spot sizes on the TLC plates. This is due to the fact that it is difficult to ionize SRB with ESI in positive ionization mode. Indeed, ESI in negative ionization mode resulted in significantly higher signal intensity for SRB, with the other cationic dyes being undetectable, however.

Figure 2 shows the liquid chromatogram (total ion chromatogram TIC) of the dialysate of the Violet pigment as an example.

For some peaks, the detected molecular m/z value matched known fluorescent dyes and optical brighteners. For confirmation, HR-MS/MS was applied. In the Q-TOF system used in this study, MS/MS works as follows: The compounds with a specific m/z value are first separated via the first mass analyzer, a quadrupole, fragmented in a collision cell with a nitrogen stream of a set energy, and the m/z values of the fragments and their ratio are then determined via the time-of-flight mass analyzer. The fragmentation reactions depend on the structure of the parent compound. Therefore, HPLC–MS/MS allows two-step unambiguous identification of compounds based on retention time and fragmentation patterns compared to

Table 1 Dyes and optical brighteners in the DFPs from Kremer Pigmente

Pigment	Rh6G	BR1:1	Rh575	BV11	BV11:1	RhB	SRB	SY172	SY44	BY40	FB184	FB61	UnkV
White											++++		
Blue		+									+	++++	
Green								++		++		+	
Lemon Yellow								+++			+++		
Golden Orange	+	++++	++	+	+			++		+	+++		
Orange		++++	++	++	+	+	+/++*	++	+	+	+++		
Brick Red	++	++++	+++	++			++/+++*	++		+	+++		
Flame Red		++++	++	++	+	+	++/+++*	+	+		+++		
Cyclamen Red	+	++++	+++	++	+	+	++/+++*				+++		
Violet		+++	+	+++	++	++	+/++*				++		++++

The semiquantitative results are labeled as follows: + in trace amounts, ++ in low amounts, +++ in medium amounts, ++++ in high amounts. *SRB showed large spots on TLC plates but low signal intensity in HPLC–MS (see Additional file 1: Fig. S1)
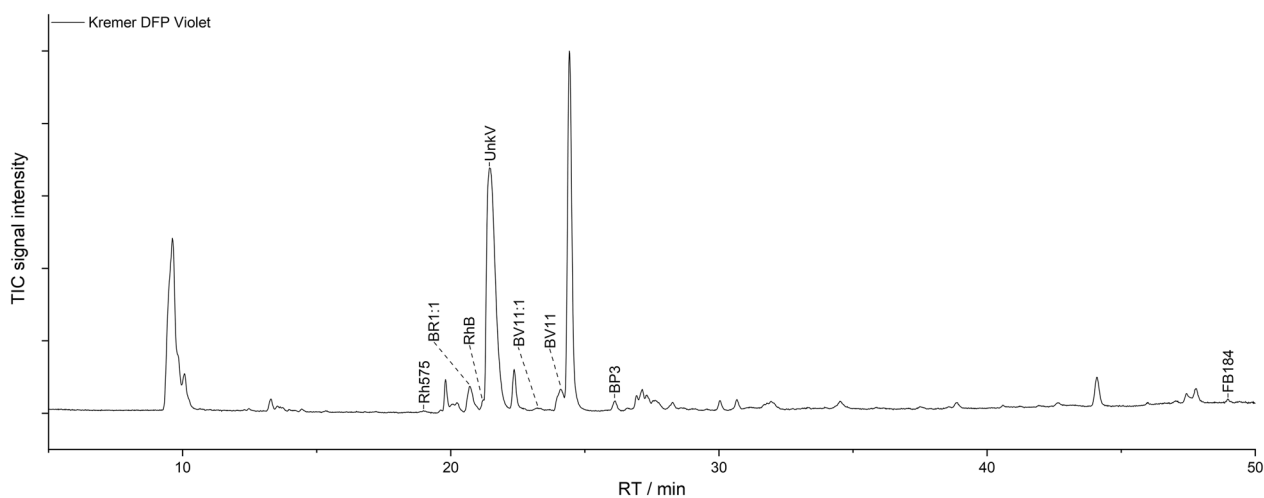
Reiß *et al. Heritage Science*   (2023) 11:146

Page 6 of 17

Fig. 2 Total ion chromatogram of the dialysate of the Violet DFP from Kremer Pigmente with marked peaks of the dyes and oxybenzone (BP3)

reference substances. In addition, the fragmentation patterns can be used to draw conclusions about the structure of unknown substances to a certain extent. MS/MS thus serves to elucidate structures. Figure 3, for example, shows the HR-MS/MS spectra of one of the main components of the Violet pigment with m/z = 471 and BV11, both appearing at a retention time of 24.1 min. The coincident mass spectra confirm BV11 as a component of the Violet DFP from Kremer Pigmente.

In this way, the dyes and optical brighteners summarized in Table 1 could be identified in the DFPs from Kremer Pigmente. A detailed listing of the retention times, mass and fragmentation pattern is provided in Additional file 1: Table S1.

The identification of the dyes in the DFPs from Kremer Pigmente in this study is largely in agreement with the results obtained by Schmidtke Sobeck et al. [8], with a few differences as discussed in "Discussion" section.

In the Orange, Brick Red, Flame Red, Cyclamen Red and Violet pigments, various representatives of both group R1 and group R2 rhodamines were detected, with BR1:1 and BV11 identified as the main components in the red color range.

With the exception of Violet and Cyclamen Red, SY172 was found as the main dye for the yellow color range in the other red and orange pigments, Lemon Yellow and Green. SY44 and BY40 were also detected in minor amounts as additional dyes in the yellow color range.
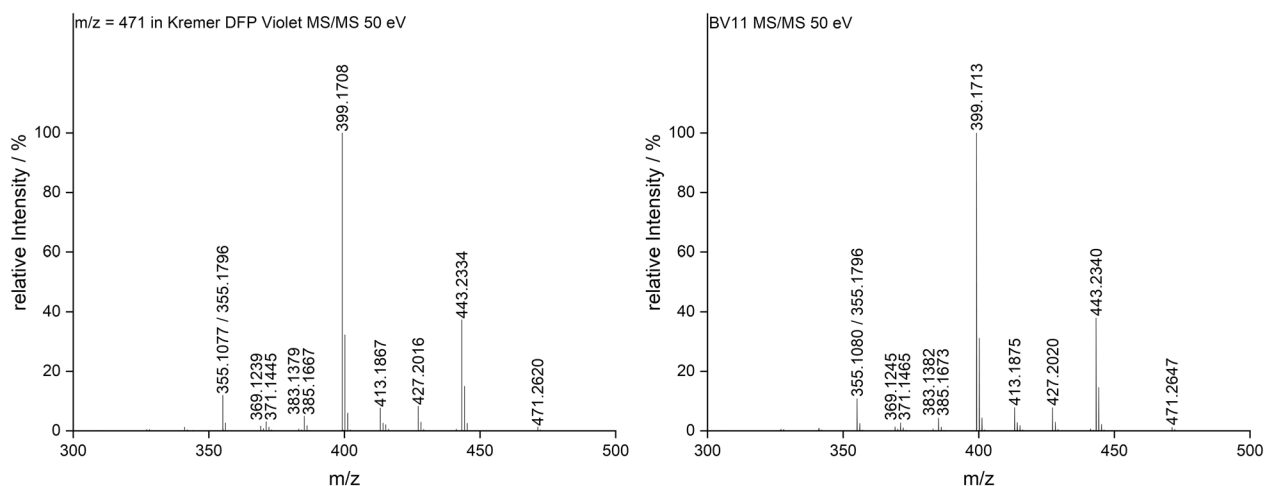

Fig. 3 HR-MS/MS spectrum of m/z = 471 in the dialysate of the Violet DFP from Kremer Pigmente with 50 eV fragmentation energy (left); HR-MS/MS spectrum of BV11 with 50 eV fragmentation energy (right)

Reiß *et al. Heritage Science*   (2023) 11:146

Page 7 of 17

FB61 was detected as an optical brightener in the Blue pigment and in trace amounts in the Green pigment. Fluorescent Brightener 184 was found in all other pigments.

In the Violet DFP, an additional violet dye (Fig. 2; UnkV) with m/z = 391.2737 was detected at a retention time of 21.5 min [8]. It is the main dye in the Violet pigment and only shows weak fluorescence on a TLC plate (see Additional file 1: Fig. S1). The exact mass matches a molecular formula of $C_{26}H_{34}N_2O + H^+/C_{26}H_{35}N_2O^+$. NMR spectroscopy revealed the structure of a cationic hemicyanine dye. HR-MS/MS confirmed the results (Fig. 4). NMR spectra are in the Additional file 1: Figs. S2 to S8.

This dye is not listed in databases such as the Colour Index, but it has a high similarity to Basic Violet 7 (BV7; Cl in place of the ethoxy group), which is known to be used in DFPs [2]. The mass of BV7 appears in the chromatogram at the same retention time as UnkV. Thus, BV7 could also be detected in low to medium amounts with m/z = 381.2081, as shown in Fig. 4.

In addition to the peaks of the dyes and optical brighteners, the chromatograms of most of the DFPs showed a peak with m/z = 229.0859 ($C_{14}H_{12}O_3 + H^+$) at 26.1 min. It probably originates from the UV absorber oxybenzone (benzophenone-3; BP3), which is known to be a component of DFPs [4, 8].

Besides the peaks of the mentioned dyes, optical brighteners and additives, intense peaks of monomers and smaller oligomers of the MSF resin appeared in the chromatograms despite the cleaning step. In Fig. 2, these are at retention times of 10 min (mainly toluenesulfonamide and oligomers), 24.4 min and between the peaks of BP3 and FB184. Some of these oligomers could only be

detected in the White DFP in very high amounts, while the reverse is true for some of the other oligomers. This confirms the assumption that a different resin was used for the White pigment.

Finally, a peak with m/z = 239.0821 ($C_{14}H_{10}N_2O_2 + H^+$) was found exclusively in the Green DFP at 19.2 min, and a peak with m/z = 236.1636 ($C_{14}H_{21}NO_2 + H^+$) was found exclusively in the Violet DFP at 22.4 min. The formulae could not be found in dye databases. They could come from additional additives. The latter possibly is 3-methylbutyl-4-(dimethylamino)benzoate (the UV absorber and photoinitiator "Padimate"; CAS 21245-01-2).

Degradation products

Figure 5 shows the ethanol solutions of the degradation products of the dyes and optical brighteners after VIS and UV aging. For BR1:1 and Rh575, the original yellow fluorescence turned greenish and that of the group 2 rhodamines shifted from red to yellow (hypsochromic shift). BY40 showed in the 10 d DL aged sample a light blue fluorescence, while the 30 d DL aged sample again has a more greenish fluorescence (Fig. 5j). However, this could also be due to differences in drying prior to aging. In summary, a visually noticeable change, significant fading and decrease in fluorescence were observed for all colorants except SY172, FB184 and FB61 during both VIS and UV aging.

Rhodamine dyes

Figure 6 shows the HPLC–MS chromatograms of the aged samples of BV11, for example. In addition to the peak of the starting substance (a, m/z = 471.2642), other peaks appear in all chromatograms (see Table 2). A
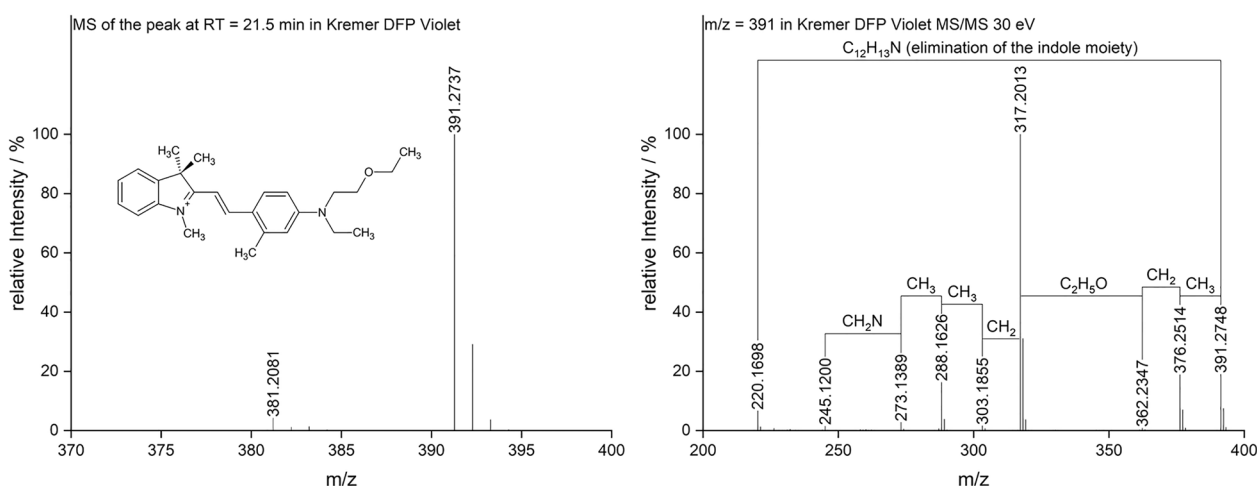

Fig. 4 HR-MS spectrum of the peak at RT = 21.5 min in the chromatogram of the dialysate of the Violet DFP from Kremer Pigmente with the proposed structure of the dye UnkV according to the results of NMR spectroscopy (left); HR-MS/MS spectrum of m/z = 391 with 30 eV fragmentation energy (right)

Reiß *et al. Heritage Science*   (2023) 11:146
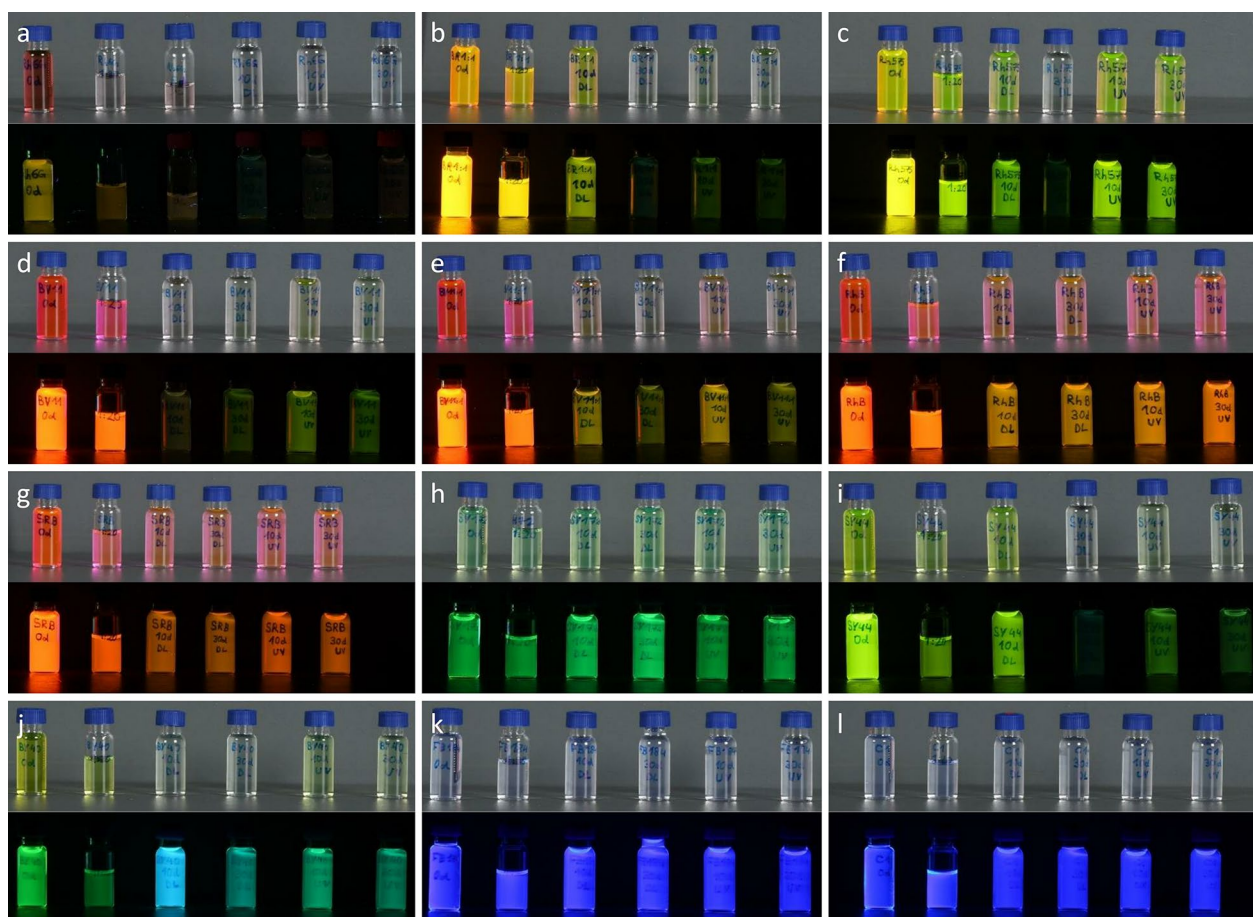
Page 8 of 17

Fig. 5 Photographs of the ethanol solutions of the aged dyes and optical brighteners; each from left to right: unaged, unaged diluted 1:20, 10 d VIS aging (5 d for Rh6G), 30 d VIS aging (10 d for Rh6G), 10 d UV aging and 30 d UV aging; DL photography above and UVF photography below; **a** Rh6G, **b** BR1:1, **c** Rh575, **d** BV11, **e** BV11:1, **f** RhB, **g** SRB, **h** SY172, **i** SY44, **j** BY40, **k** FB184, **l** FB61
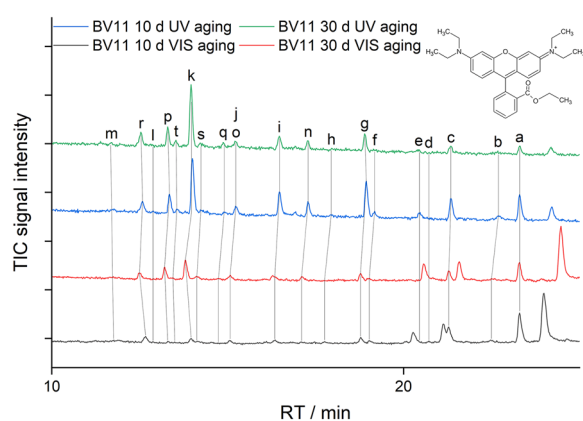

Fig. 6 Chromatogram of the aged samples of BV11 with labeled peaks of major degradation products. The retention time was normalized on peak a. Shift of retention time between measurements occurred due to cleaning of the device and column change between measurements of VIS aged samples and UV aged samples. Some peaks (for example the intense peak at about 24 min) are not labeled and are presumably from column bleeding

summary of the degradation products of all dyes and optical brighteners found with HPLC–HR-MS is given in Additional file 1: Table S2.

N-deethylation and dealkylation For the rhodamines (Rh6G, BR1:1, Rh575, BV11, BV11:1, RhB and SRB), the main degradation products are the deethylated products with a mass difference of $\Delta m/z = 28$ (for BV11: $m/z = 471 \rightarrow 443 \rightarrow 415 \rightarrow 387 \rightarrow 359 \rightarrow 331$). This is consistent with the findings in the literature [16–18], which demonstrated complete N-deethylation for RhB during light aging. Results from the literature show that for RhB two peaks appear in the chromatogram for the twice N-deethylated product due to isomers. This is also confirmed in our study for RhB (Additional file 1: Table S2). For BV11, the deethylation is more complex because it can occur at both of the nitrogen atoms and the ester. The first deethylation step ($m/z = 443.2329$, $C_{28}H_{31}N_2O_3^+$) indeed shows two peaks (c and d). Peak d comes from RhB according to its HR-MS/MS spectrum. Following from the signal intensity, the N-deethylated

Table 2 Degradation products of BV11 found with HPLC–HR-MS

Peak label	Exact mass	Molecular formula	Abundance	Degradation type
a	471.2642	$C_{30}H_{35}N_2O_3^+$		Starting substance
b	457.2486	$C_{29}H_{33}N_2O_3^+$	+	Dealkylation/impurity
c, d	443.2329	$C_{28}H_{31}N_2O_3^+$	++	N-deethylation
e	429.2173	$C_{27}H_{29}N_2O_3^+$	+	Dealkylation/impurity
f, g	415.2016	$C_{26}H_{27}N_2O_3^+$	++	N-deethylation
h	401.1860	$C_{25}H_{25}N_2O_3^+$	+	Dealkylation/impurity
i	387.1703	$C_{24}H_{23}N_2O_3^+$	++	N-deethylation
j	373.1547	$C_{23}H_{21}N_2O_3^+$	+	Dealkylation/impurity
k	359.1390	$C_{22}H_{19}N_2O_3^+$	++	N-deethylation
l	345.1234	$C_{21}H_{17}N_2O_3^+$	+	Dealkylation/impurity
m	331.1077	$C_{20}H_{15}N_2O_3^+$	+	Deethylation
	487.2591	$C_{30}H_{35}N_2O_4^+$	+	Hydroxylation
	459.2278	$C_{28}H_{31}N_2O_4^+$	+	Hydroxylation/N-deethylation
	445.2122	$C_{27}H_{29}N_2O_4^+$	+	Hydroxylation/dealkylation
	431.1965	$C_{26}H_{27}N_2O_4^+$	+	Hydroxylation/N-deethylation
	403.1652	$C_{24}H_{23}N_2O_4^+$	+	Hydroxylation/N-deethylation
	389.1496	$C_{23}H_{21}N_2O_4^+$	+	Hydroxylation/dealkylation
	375.1339	$C_{22}H_{19}N_2O_4^+$	+	Hydroxylation/N-deethylation
n	457.2122	$C_{28}H_{29}N_2O_4^+$	++	Oxidation/N-deethylation
	443.1965	$C_{27}H_{27}N_2O_4^+$	+	Oxidation/dealkylation
o	429.1809	$C_{26}H_{25}N_2O_4^+$	+	Oxidation/N-deethylation
	415.1652	$C_{25}H_{23}N_2O_4^+$	+	Oxidation/dealkylation
p, q	401.1496	$C_{24}H_{21}N_2O_4^+$	+	Oxidation/N-deethylation
r	387.1339	$C_{23}H_{19}N_2O_4^+$	+	Oxidation/dealkylation
	501.2384	$C_{30}H_{33}N_2O_5^+$	+	Oxidation
	473.2071	$C_{28}H_{29}N_2O_5^+$	+	Oxidation/N-deethylation
s, t	443.1601	$C_{26}H_{23}N_2O_5^+$	+	Oxidation/N-deethylation

Abundance: + minor, ++ major

product (peak c) is strongly preferred. Therefore, just as with RhB, the second (m/z = 415.2016, $C_{26}H_{27}N_2O_3^+$) and third (m/z = 387.1703, $C_{24}H_{23}N_2O_3^+$) deethylation steps show only two peaks (f and g) and one peak (i), respectively. Accordingly, the fourth deethylation step (m/z = 359.1390, $C_{22}H_{19}N_2O_3^+$) also shows only one peak (k) from the N,N,N',N'-tetra-deethylated product. The results for BV11 show that the ethyl group at the ester is degraded in the fifth step, too. The signal intensity of the fully deethylated BV11 (m, m/z = 331.1077, $C_{20}H_{15}N_2O_3^+$) is very weak, as deethylation at the ester group appears to be very unlikely. Regarding the dealkylated products of the rhodamines, it should be noted that peaks with a mass difference of Δm/z = 14 were found (b, e, h, j and l, see Table 2), but with lower peak area than the deethylated products (mainly in noise). It can be assumed that these are predominantly due to impurities (other substituted derivatives) of the starting materials rather than demethylenated products. This is supported by the fact that the unaged BV11 already contains BV11:1

(about 10% of the peak area) as well as RhB (which is of course also one of the degradation products of BV11). Conversely, the unaged sample of BV11:1 also contains BV11 (about 17% of the peak area). In addition, SRB only shows the products with Δm/z = 28, since there are no different esters. On the other hand, for the group R1 rhodamines, two peaks with m/z = 415.2016 appear for BR1:1 (m/z = 429.2173, $C_{27}H_{29}N_2O_3^+$), but no Rh6G (m/z = 443.2329, $C_{28}H_{31}N_2O_3^+$) as impurity, which could lead to the two different products with m/z = 415.2016 upon deethylation. The same is true for Rh575, which has no BR1:1 impurity and yet has a degradation product with m/z = 401.1860. Thus, it seems that to a small extent a release of methylene groups actually takes place during degradation.

Oxidation In addition to the deethylated products, other degradation products were found in the chromatograms (see Table 2), some of these in the same order of magnitude as the deethylated products according to the peak area. Many of the exact masses of molecular

Reiß *et al. Heritage Science*   (2023) 11:146

Page 10 of 17

ions given show multiple peaks in the chromatograms. According to the molecular formulae, these degradation products are mainly oxidation products. Of course, there are numerous combinations of deethylation and oxidation leading to many other products detected in trace amounts and not labelled in Fig. 6. Higher oxidized products, such as aldehydes and ketones, could also be found (see Table 2).

To determine where oxygen is incorporated in the molecular structure, HPLC–HR-MS/MS was performed on the oxidation products of RhB with m/z=459.2278 ($C_{28}H_{31}N_2O_4^+$). RhB was chosen because of many different oxidation products and the HR-MS/MS fragmentation pattern of RhB is well elucidated [28]. Figure 7 shows the extracted ion current (EIC) of m/z=459.2278 in the chromatogram of RhB after 10 d VIS aging.

Eight different degradation products with additional oxygen could be found (1 to 8). Figure 8 compares their HR-MS/MS spectra with the HR-MS/MS spectrum of RhB.

As noted in the literature [28], the N-ethyl groups (mainly as C_2H_6 and C_3H_8 via radical mechanism), the nitrogen atoms (as $CH_2N\cdot$ radical after cleavage of C_3H_8) and the carboxyl group (as CO_2) are released during the fragmentation of RhB (at similar fragmentation energy to [28]). Besides the fragments from the cleavage of C_2H_6 (m/z=429.1808, $C_{26}H_{25}N_2O_4^+$) and C_3H_8 (m/z=415.1652, $C_{25}H_{23}N_2O_4^+$), the products belonging to peaks 1, 2 and 3 (Fig. 8 b, c, d) show fragments from the cleavage of C_2H_6O (m/z=413.1860, $C_{26}H_{25}N_2O_3^+$) and C_3H_8O (m/z=399.1703, $C_{25}H_{23}N_2O_3^+$) followed by the loss of the $CH_2N\cdot$ radical (m/z=371.1516, $C_{24}H_{21}NO_3^+$). Accordingly, these peaks belong to substances where oxidation has occurred at the N-ethyl groups.
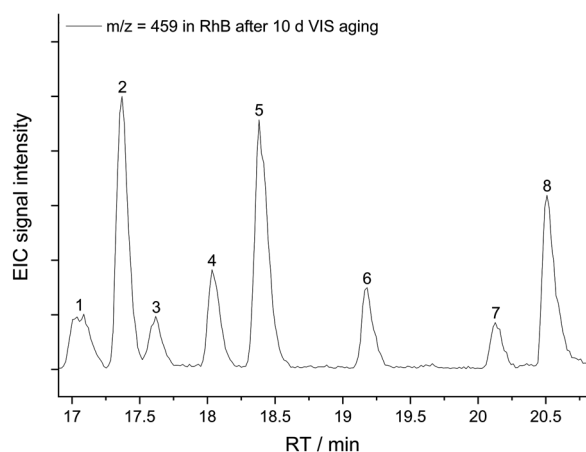
The oxidation products of RhB belonging to peaks 4 and 6 (Fig. 8e, g) have the same fragmentation patterns with similar intensity ratios as RhB. Therefore, the oxidation did not take place at a site affected by this fragmentation mechanism. Presumably, the oxygen atom was added to the aromatic rings as a hydroxyl group.

For the compounds belonging to peaks 5, 7 and 8 (Fig. 8f, h, i), no clear information can be derived from the HR-MS/MS data. For these peaks, however, many fragments with a mass of m/z < 300 could be found, suggesting that the rhodamine framework is destroyed during fragmentation and thus it is probably involved in oxidation.

The proposed degradation pathways of rhodamines found in this study are summarized in Fig. 9. All degradation products could be found under VIS aging as well as under UV aging, similarly after 10 d and 30 d aging. For the deethylated products, the ratios of the peak areas 30 d/10 d increased as deethylation progressed, for both VIS and UV aging.

Coumarin dyes

N-deethylation also occurred in the coumarin dyes (SY172, BY40 and FB61). In fact, for SY172 (m/z=414.1118, $C_{20}H_{20}N_3O_5S^+$) the deethylated products (m/z=386.0805, $C_{18}H_{16}N_3O_5S^+$ and m/z=358.0492, $C_{16}H_{12}N_3O_5S^+$) were the only degradation products found by HPLC–HR-MS in trace amounts and the color of SY172 was quite stable to VIS and UV aging (Fig. 5h). The sulfonamide group appears to prevent reactions at the benzoxazole substituent either sterically or due to its electron-withdrawing effect.

FB61 (m/z=232.1332, $C_{14}H_{18}NO_2^+$) was affected by both VIS and UV aging. The main degradation products were also the N-deethylated products (m/z=204.1019, $C_{12}H_{14}NO_2^+$ and m/z=176.0706, $C_{10}H_{10}NO_2^+$). Furthermore, a degradation product was found with two missing carbon atoms compared to FB61 (m/z=208.1332, $C_{12}H_{18}NO_2^+$). The proposed structure based on the HR-MS/MS results is shown in Fig. 10. Other degradation products were oxidation products such as hydroxylation products (m/z=248.1281, $C_{14}H_{18}NO_3^+$) and the corresponding aldehydes and ketones (m/z=218.0812, $C_{12}H_{12}NO_3^+$), also shown in Fig. 10.

The degradation products of BY40 (m/z=362.1863, $C_{22}H_{24}N_3O_2^+$) were again N-deethylated products (m/z=334.1550, $C_{20}H_{20}N_3O_2^+$ and m/z=306.1237, $C_{18}H_{16}N_3O_2^+$), hydroxylation products (m/z=378.1812, $C_{22}H_{24}N_3O_3^+$), aldehydes and ketones (m/z=348.1343, $C_{20}H_{18}N_3O_3^+$). The hydroxylation products showed a greater variety than for FB61. The absence of the characteristic benzimidazolium fragment (m/z=145.0760, $C_9H_9N_2^+$) and instead the presence of a fragment with
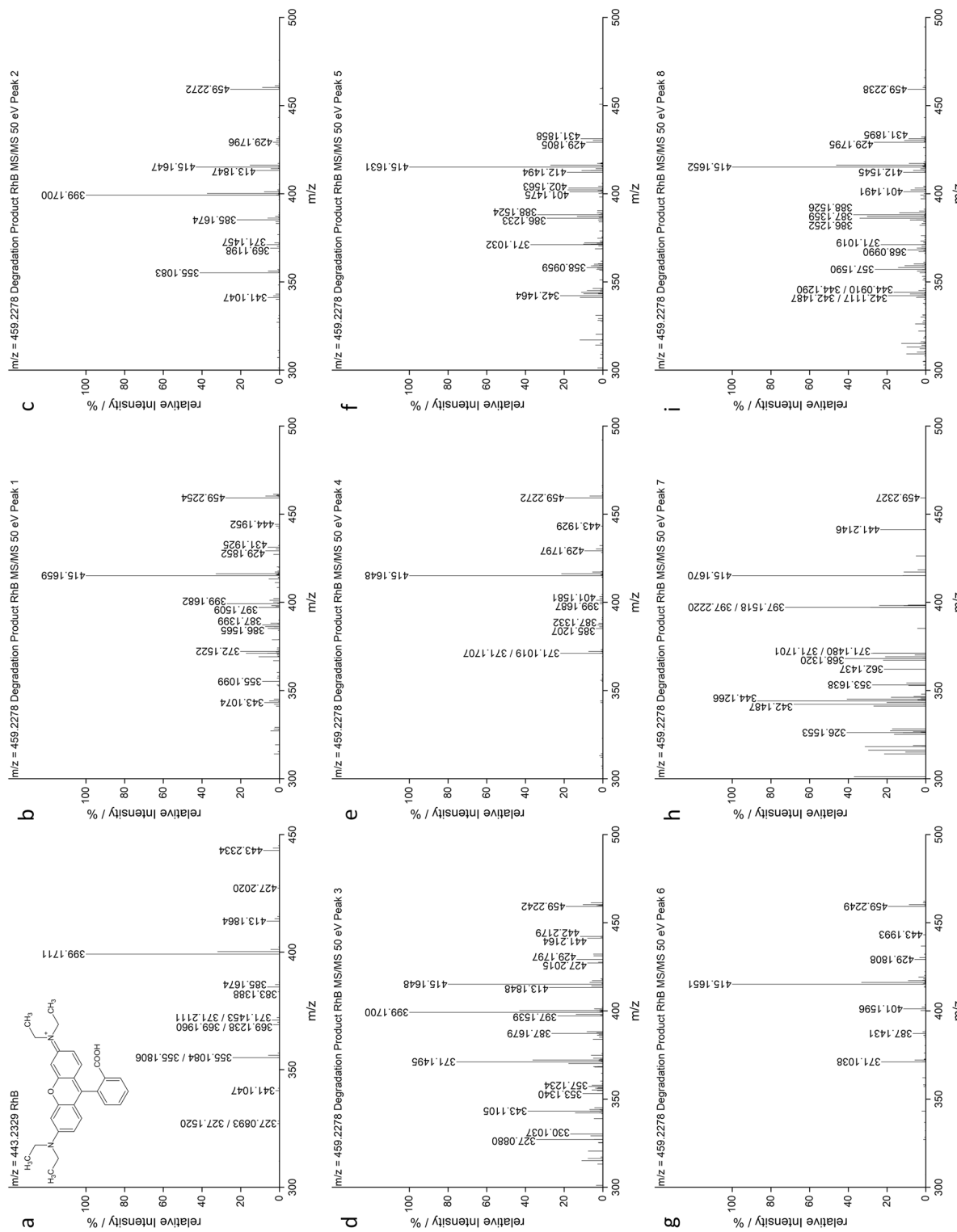
Fig. 7 Extracted ion chromatogram of m/z=459.2278 in the sample of RhB after 10 d VIS aging

Fig. 8 HR-MS/MS spectra of RhB and its degradation products with additional oxygen; **a** RhB, **b** peak 1, **c** peak 2, **d** peak 3, **e** peak 4, **f** peak 5, **g** peak 6, **h** peak 7, **i** peak 8
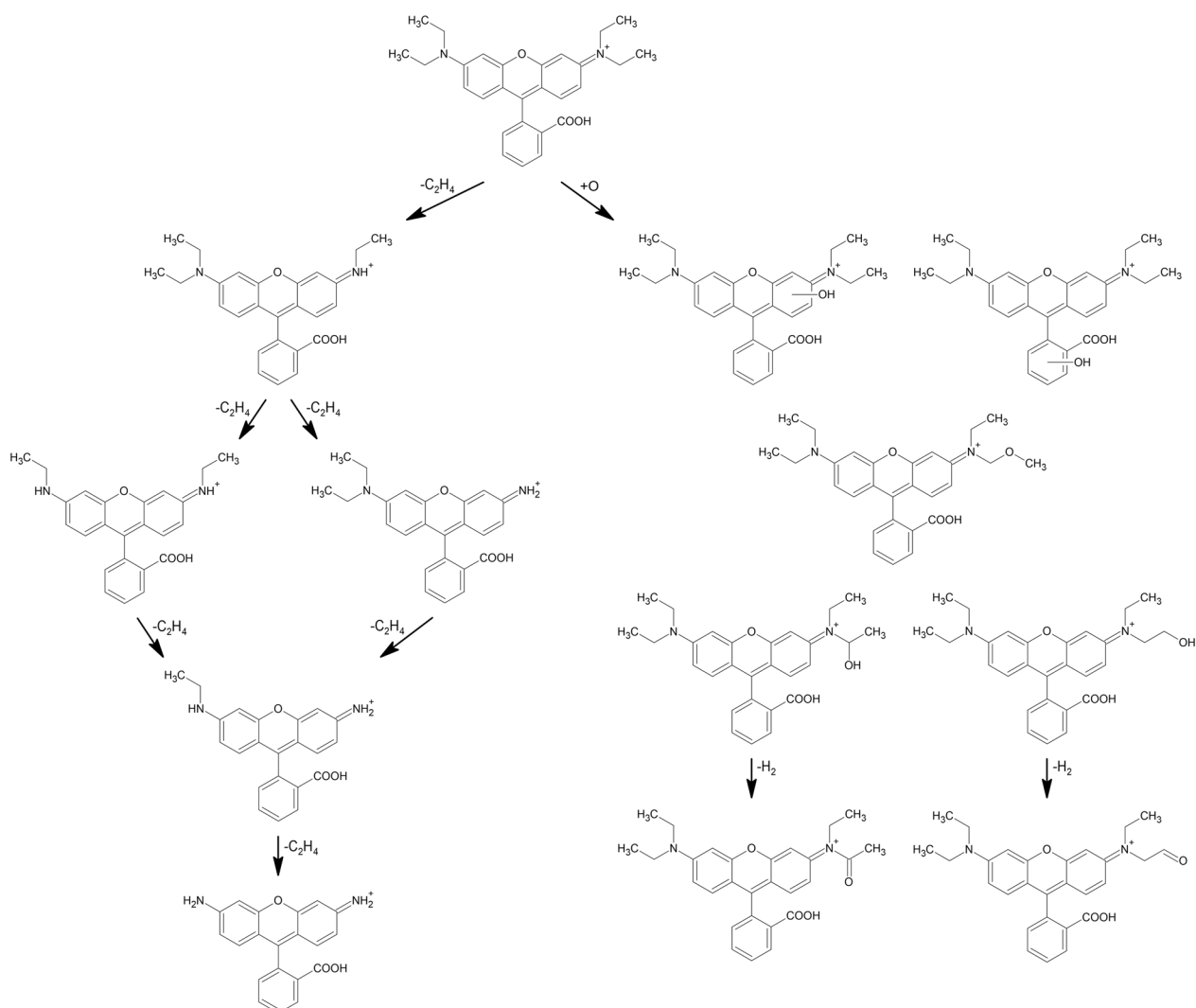
Reiß *et al. Heritage Science*   (2023) 11:146

Page 12 of 17

Fig. 9 Proposed degradation pathways of rhodamines using RhB as an example, determined by HPLC–HR-MS/MS

m/z = 161.0709 ($C_9H_9N_2O^+$) in the HR-MS/MS spectra of some of the hydroxylated products indicates hydroxylation of the benzimidazole moiety of BY40. For BY40, other degradation products with more than one additional oxygen atoms (e. g. m/z = 394.1761, $C_{22}H_{24}N_3O_4^+$) also appeared, as well as a product with one nitrogen missing (m/z = 319.1441, $C_{20}H_{19}N_2O_2^+$), indicating cleavage of the benzimidazole moiety. As can be seen in Fig. 5j, specifically VIS aging had a very strong effect on BY40 compared to the other coumarins, visible through fading of the solution and a blue shift in fluorescence. As for the rhodamines, all degradation products of the coumarins were produced under both VIS aging and UV aging.

Solvent Yellow 44 and Fluorescent Brightener 184
The aminonaphthalimide dye SY44 (m/z = 317.1285, $C_{20}H_{17}N_2O_2^+$) was very strongly degraded under VIS

and UV aging (Fig. 5i). Although the signal intensity of the starting material decreased rapidly, HPLC–HR-MS revealed only weak signals from numerous hydroxylated products (m/z = 333.1234, $C_{20}H_{17}N_2O_3^+$) and one product with a missing nitrogen (m/z = 302.1176, $C_{20}H_{16}NO_2^+$), the latter already present in the unaged sample.

The chromatograms of the degraded samples of FB184 (m/z = 431.1788, $C_{26}H_{27}N_2O_2S^+$) did not show any additional peaks. Even if not clearly visible from the photograph (Fig. 5k), degradation nevertheless occurred. FB184 was the only one among the investigated substances for which UV aging caused significantly more rapid degradation than VIS aging under the conditions of the experiment, as its signal intensity decreased more during UV aging.
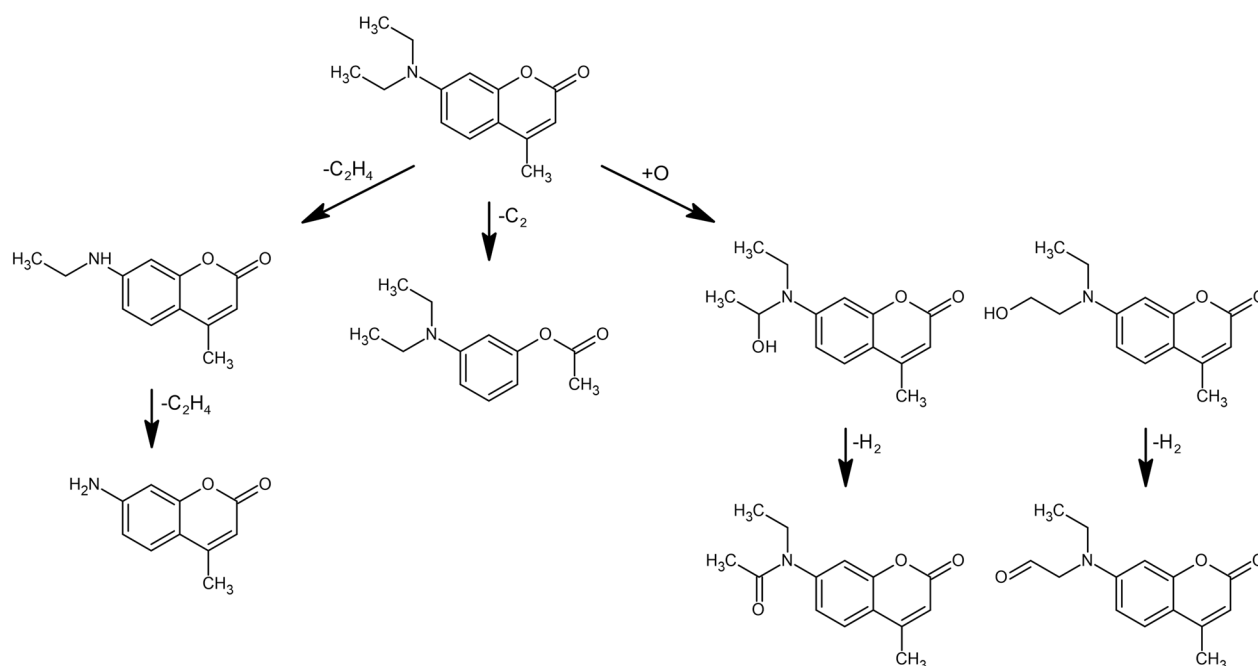
Fig. 10 Proposed degradation pathways of FB61, determined by HPLC–HR-MS/MS

Identification of the degradation products in aged paint samples

The investigated samples of aged paint mock-ups [13] include the entire range of dyes and optical brighteners in Kremer DFPs (see Table 1) except SY44. The dyes and optical brighteners and their degradation products found in the samples are summarized in Table 3.

Except for all degradation products of FB61 in the Blue paint sample, only very few of the degradation products could be found in the samples of the aged paint mockups. Possible reasons are given in the following section.

Discussion

In the Kremer DFPs, we found BR1:1, Rh575, BV11, SY172, FB184, FB61 and a hemicyanine dye similar to BV7 as the main components and Rh6G, BV11:1, RhB, SRB, SY44 and BY40 as minor components depending on the color tone of the DFP. These results are largely in agreement with the findings in the HPLC–DAD–MS study by Schmidtke Sobeck et al. [8]. Minor differences are that in the present study some dyes were found in traces that could not be detected by Schmidtke Sobeck et al. [8], probably due to the lower detection limit of our

Table 3 Dyes and optical brighteners and their degradation products found in paint samples

Molecular formula	Origin (degradation)	Blue UV aged	Lemon Yellow VIS aged	Brick Red VIS aged	Violet VIS aged
$C_{27}H_{29}N_2O_3^+$	BR1:1			++	+
$C_{25}H_{25}N_2O_3^+$	BR1:1 $(-C_2H_4)$			++	+
$C_{30}H_{35}N_2O_3^+$	BV11				+
$C_{14}H_{18}NO_2^+$	FB61	+++			
$C_{12}H_{14}NO_2^+$	FB61 $(-C_2H_4)$	+++			
$C_{10}H_{10}NO_2^+$	FB61 $(-C_4H_8)$	++			
$C_{12}H_{18}NO_2^+$	FB61 $(-C_2)$	+++			
$C_{14}H_{18}NO_3^+$	FB61 $(+O)$	++			
$C_{12}H_{12}NO_3^+$	FB61 $(-C_2H_6; +O)$	+			
$C_{11}H_{10}NO_3^+$	FB61 $(-C_3H_8; +O)$	+			
$C_{26}H_{27}N_2O_2S^+$	FB184	++	+++	+++	++

The semiquantitative results are labeled as follows: + in trace amounts, ++ in low amounts, +++ in medium amounts

Reiß *et al. Heritage Science* (2023) 11:146

Page 14 of 17

instrument. These are BV11:1, RhB (although in higher concentrations in the Violet pigment), BY40, FB184 in the Violet pigment and SY44.

Schmidtke Sobeck et al. [8] did not detect Rh575, which was found in medium amounts in several pigments in the present study. Probable reasons are high in-source fragmentation in their study and much easier fragmentation of Rh575 compared to Rh6G (Additional file 1: Table S1). Due to the high signal intensity, it seems less likely that the Rh575 found in the present study is just a synthetic byproduct or precursor in the synthesis of BR1:1. Parts of the Rh575 are also a degradation product of BR1:1.

It is important to note that rhodamines from bulk suppliers are more heavily contaminated with other esters than products from fine chemical suppliers, either for production reasons or due to prolonged storage. Therefore, it is quite possible that the complex rhodamine composition in DFPs demonstrated in this study and by Schmidtke Sobeck et al. [8] was not intended by the manufacturer, but was the result of impurities in the raw materials. In particular, the detection of RhB in trace amounts in all the red colored DFPs could be explained in this way.

Schmidtke Sobeck et al. [8] assumed that a yellow dye in historic pigment samples from DayGlo Color Corp. is the coumarin dye Solvent Yellow 135 (SY135). However, they were unable to confirm this because the reference substance they acquired turned out to be SY172. The CAS number they give for SY135 (CAS 144246-02-6) and the neutral mass of 316 g/mol lead to a structure consistent with that of SY44 (CAS 2478-20-8) used in the present study. Thus, we see the assumption of Schmidtke Sobeck et al. confirmed, but would like to note that this structure is not a coumarin dye but an aminonaphthalimide.

In the present study, the structure of the unknown violet dye UnkV mentioned by Schmidtke Sobeck et al. [8] in the Violet pigment could be elucidated by NMR spectroscopy. The structure is similar to the hemicyanine dye BV7, which was also found in small amounts. Perhaps, BV7 was replaced by UnkV by the manufacturer of the pigment either because of better properties or as a trade secret.

In addition to the dyes and optical brighteners, the UV absorber BP3 was found in the same pigments as stated in [8]. Álvarez-Martín et al., on the other hand, were able to detect BP3 in the White DFP from Kremer Pigmente, too, which was the only pigment from Kremer Pigmente in the GC–MS part of their study [4]. This is somewhat surprising, because as described in Sect. 2.2, the White pigment has a much higher solubility than the other pigments and BP3 should therefore have been detected by HPLC–HR-MS in our study, even if it is only present in trace amounts. In addition, Álvarez-Martín et al. also

found BP3 in historical DayGlo pigment samples from the private collection of Herbert Aach [4]. Schmidtke Sobeck et al. could only detect BP3 in their samples from Radiant Color and Kremer Pigmente (Radiant Color supplies the pigments to Kremer Pigmente), but not in the modern pigments from DayGlo [8]. Accordingly, the use of UV absorbers also appears to have changed during the production history of DFPs.

For the identification of the degradation products, dry reference substances of the dyes and optical brighteners were aged photochemically in air, both under visible light and with UV radiation, and analyzed with HPLC–HR-MS/MS.

For the rhodamine dyes, the main degradation pathways identified by HPLC–HR-MS/MS were N-deethylation, hydroxylation and higher oxidation. Dealkylation at the ester group occurs only to a small extent. In addition to the reduction of the concentration of the original dye [9, 12], the deethylated products are probably mainly responsible for the change of the fluorescence color. The loss of the electron-donating effect of the N-ethyl groups leads to an increase in the energy gap between electronic ground state and excited state, resulting in the hypsochromic shift. N-deethylation of RhB in aqueous solution in presence of different catalysts has been studied previously by Yu et al. [16], He et al. [17] and Natarajan et al. [18]. Other degradation products found in these studies were smaller molecules resulting from the cleavage of the chromophore system, such as terephthalic acid or adipic acid, identified by GC–MS. In the present study, none of these fragments could be detected by HPLC–MS (even in negative ionization mode). However, the light aging carried out in air probably led to increased oxidation. The primary oxidation products of the rhodamine structure found in our study can be regarded as precursors to the cleavage of the chromophore system. The rhodamines degraded under both visible light and UV radiation. Based on the degradation products, it is difficult to distinguish between the different rhodamines except SRB for small samples with HPLC–HR-MS/MS, because rhodamines share the degradation products, even group R1 and group R2 rhodamines.

Similar to the rhodamine dyes, the degradation products identified for coumarins were N-deethylation products as well as oxidation products. However, the different substituents on the three coumarins studied had a significant effect on the degradation rate and the nature of the degradation products. SY172 was found to be stable to oxidation. FB61 showed oxidation products of the N-ethyl group as well as cleavage of the chromophore system. Studies on the degradation products of FB61 in a laser by Winters et al. [20] showed that oxidation occurs at the methyl substituent. In our measurements, however,

the typical cleavage of the N-ethyl groups could no longer be observed for the oxidized products. Therefore, oxidation is assumed at the N-ethyl groups. For BY40, we found that the benzimidazole substituent is much more susceptible to oxidation than the benzoxazole substituent from SY172, which led to a significant degradation of BY40 during our experiment.

The aminonaphthalimide dye SY44 showed strong degradation, but only small amounts of hydroxylated products were found by HPLC–HR-MS. It is obvious that other advanced degradation products must have been formed, but these could not be detected by our method. FB184 was found to be relatively stable to VIS aging but susceptible to UV radiation. However, again no degradation products could be identified by HPLC–HR-MS.

In the aged paint samples, only a few of the degradation products could be identified. It should be noted, however, that these paints were aged much longer than the dye samples in the present study to the point where Raman spectroscopy could no longer detect the originally contained dyes [13]. These analyses therefore only provide information on whether the degradation products can still be identified at an advanced stage of aging. Although it is possible that the concentration of the degradation products in the paint samples was simply too low, the example of the Blue paint sample, in which all degradation products of FB61 could be found, shows that the degradation products can definitely be detected. It can therefore be assumed that the aging of the other samples was simply too far advanced. The paint mock-ups have been aged under elevated exposure compared to the dyes (at least 5.8 times for VIS and 2.2 times for UV aging).

In order to draw conclusions for appropriate conservation handling of daylight fluorescent paints, the authors propose to investigate the degradation products formed in an oxygen-free atmosphere. Subsequently, the potential effect of oxygen-free storage could be estimated. Colorimetric studies [29] and Microfading studies [30] already suggested that anoxic conditions have no significant effect on the aging rate of daylight fluorescent paints, which is surprising with respect to the oxidation products in this study. On the other hand, it is of course possible that due to the reduced oxygen diffusion in the MSF resin, significantly less oxidation occurs in the DFPs than in the pure dyes and optical brighteners.

Summary and conclusions
The present study is divided into three parts: the identification of dyes and optical brighteners in the DFP palette from Kremer Pigmente, the analysis of their degradation products, and the identification of the degradation products in aged paint samples.

A novel method for separating the resin of DFPs from the dyes and optical brighteners by dialysis is presented. It revealed more complete separation of all colorants from the resin compared to other approaches such as solid phase extraction [24]. The samples obtained were analyzed by HPLC–HR-MS/MS and the colorants were successfully identified. The results extend the findings on colorant composition in DFPs from previous studies [6–8]. An additional rhodamine dye (Rh575) and the presumed yellow dye SY44 [8] were found by HPLC–MS/MS, and the structure of the violet dye in the violet DFP from Kremer Pigmente was elucidated using NMR spectroscopy. BP3 was confirmed as an additive used in the production of DFPs and assumptions were made about other additives.

With respect to the degradation products, mainly N-deethylation (if applicable), hydroxylation and higher oxidation could be identified as major degradation pathways for all found colorant classes. Although studies showed that anoxic conditions do not lead to a significant slowing of the aging process of daylight fluorescent paints [29, 30], the authors recommend that studies be conducted on the degradation products that result from photochemical aging in the absence of oxygen. Upon photochemical aging in air, all colorants were degraded in both VIS and UV aging, with only FB184 being significantly more susceptible to UV aging.

Due to the advanced state of aging, only very few of the determined degradation products could still be detected in the aged paint. Nevertheless, the study shows the potential of the analytical methods used (especially HPLC–MS/MS) for the analysis of artworks where possibly DFPs have been used but are no longer visible due to degradation.

Abbreviations

HPLC	High-performance liquid chromatography
HR	High-resolution
ESI	Electrospray ionization
MS/MS	Tandem mass spectrometry
DFP	Daylight fluorescent pigment
MSF resin	Melamine toluenesulfonamide formaldehyde resin
TLC	Thin-layer chromatography
SERS	Surface-enhanced Raman spectroscopy
DAD	Diode array detector
PG7	Pigment Green 7
PB15:3	Pigment Blue 15:3
SRB	Sulforhodamine B
BV11	Basic Violet 11
BV11:1	Basic Violet 11:1
BY40	Basic Yellow 40
SY44	Solvent Yellow 44
SY172	Solvent Yellow 172
Rh6G	Rhodamine 6G
Rh575	Rhodamine 575
RhB	Rhodamine B
FB184	Fluorescent Brightener 184
BR1:1	Basic Red 1:1

Reiß *et al. Heritage Science*   (2023) 11:146

Page 16 of 17

FB61	7-Diethylamino-4-methylcoumarin
DL photography	Visible light photography
UVF photography	UV-induced visible fluorescence photography
ACN	Acetonitrile
NMR Spectroscopy	Nuclear magnetic resonance spectroscopy
Q-TOF	Quadrupole time-of-flight
BP3	Oxybenzone
UnkV	Unknown violet dye
BV7	Basic Violet 7
TIC	Total ion current
EIC	Extracted ion current

Supplementary Information

The online version contains supplementary material available at https://doi.org/10.1186/s40494-023-00993-6.

> **Additional file 1** Supporting Tables and Figures.

Availability of data and materials
The data generated or analyzed during this study are either included in this published article and its supplementary information files or are available from the corresponding author on reasonable request.

Declarations

Competing interests
The authors declare that they have no competing interests.

References
1. Deiss A. Das Gegenteil von zurückhaltend: Tagesleuchtfarben in der Kunst. In: Deiss A, Jahn A, Schimpf S, editors. Neon – Vom Leuchten der Kunst. Köln: Wienand Verlag; 2013. p. 10–25.
2. Christie RM. Fluorescent dyes. Rev Prog Coloration. 1993;23:1–18.
3. Streitel SG. Fluorescent pigments (daylight). In: Ley C, de Azevedo DCS, Bell TA, El-Halwagi M, Gong J, Jiménez-Gonzáles C, Kister H, Powell JB, Soares JBP, Teich C, editors. Kirk-Othmer encyclopedia of chemical technology. New York: Wiley; 2009. pp. 584–608.
4. Álvarez-Martín A, De Winter S, Nuyts G, Hermans J, Janssens K, Van der Snickt G. Multi-modal approach for the characterization of resin carriers in daylight fluorescent pigments. Microchem J. 2020;159:105340.
5. Fremout W, Saverwyns S. Characterization of daylight fluorescent pigments in contemporary artists' paints by Raman spectroscopy. In: IRUG 11 conference; 2014; Boston. pp. 1–5.
6. Boscacci M, Francone S, Galli K, Bruni S. The brightest colors: A Fourier-transform Raman, surface-enhanced Raman, and thin-layer chromatography-surface-enhanced-Raman spectroscopy study of fluorescent artists' paints. J Raman Spectrosc. 2020;51:1108–17.
7. Campanella B, Botti J, Cavaleri T, Cicogna F, Legnaioli S, Pagnotta S, et al. The shining brightness of daylight fluorescent pigments: Raman and SERS study of a modern class of painting materials. Microchem J. 2020;152:104292.
8. Schmidtke Sobeck SJ, Chen VJ, Smith GD. Shedding Light on Daylight Fluorescent Artists' Pigments, Part 1: Composition. J Am Inst Conserv. 2021;61:218–36.
9. Connors-Rowe S, Morris HR, Whitmore P. Evaluation of appearance and fading of daylight fluorescent watercolors. J Am Inst Conserv. 2005;44:75–94.
10. Kubik M. The use of non-sampling spectroscopic techniques in conservation: improved methodologies for pigment identification. PhD Thesis, Research School of Chemistry, Australian National University, Canberra; 2006.
11. Yoshizawa A. Daylight fluorescent pigments in works of art: properties, history, and fading. Master's Thesis, Department of Art, Queens University, Ontario; 2000.
12. Hinde E. A spectroscopic and chromatographic study of the photochemical properties of daylight fluorescent paint. PhD Thesis, School of Historical Studies and School of Physics, University of Melbourne, Melbourne; 2009.
13. Reiß L, Prestel T, Giering S. The light aging behavior of daylight fluorescent paints: a colorimetric, photographic, Raman spectroscopic and fluorescence spectroscopic study. Herit Sci. 2022;10:171.
14. Gessner T, Mayer U. Triarylmethane and diarylmethane dyes. In: Ley C, Elvers B, Bellussi G, Bus J, Greim H, Hessel V, Jeschke P, Kleemann A, Kutscher B, Meijer G, Moran S, Mukherjee J, Palkovits R, Pfaendner R, Qiao G, Sundmacher K, Teles JH, Ulber R, Wagemann K, Wietelmann U, editors. Ullmann's encyclopedia of industrial chemistry. New York: Wiley-VCH; 2000. pp. 425–78.
15. Maheshwari K, Agrawal M, Gupta AB. Dye pollution in water and wastewater. In: Muthu SS, Khadir A, editors. Novel materials for dye-containing wastewater treatment. Singapore: Springer Singapore; 2021. p. 1–25.
16. Yu K, Yang S, He H, Sun C, Gu C, Ju Y. Visible light-driven photocatalytic degradation of rhodamine B over NaBiO3: pathways and mechanism. J Phys Chem A. 2009;113:10024–32.
17. He Z, Sun C, Yang S, Ding Y, He H, Wang Z. Photocatalytic degradation of rhodamine B by Wi2WO6 with electron accepting agent under microwave irradiation: Mechanism and pathway. J Hazard Mater. 2009;162:1477–86.
18. Natarajan TS, Thomas M, Natarajan K, Bajaj HC, Tayade RJ. Study on UV-LED/TiO2 process for degradation of Rhodamine B dye. Chem Eng J. 2011;169:126–34.
19. Ismael R, Schwander H, Hendrix P. Fluorescent Dyes and Pigments. In: Ley C, Elvers B, Bellussi G, Bus J, Greim H, Hessel V, Jeschke P, Kleemann A, Kutscher B, Meijer G, Moran S, Mukherjee J, Palkovits R, Pfaendner R, Qiao G, Sundmacher K, Teles JH, Ulber R, Wagemann K, Wietelmann U, editors. Ullmann's encyclopedia of industrial chemistry. New York: Wiley-VCH; 2013. pp. 1–22.
20. Winters BH, Mandelberg HI, Mohr WB. Photochemical products in coumarin laser dyes. Appl Phys Lett. 1974;25:723–5.
21. Jones G II, Bergmark WR. Photodegration of Coumarin laser dyes: an unexpected singlet self-quenching mechanism. J Photochem. 1984;26:179–84.
22. Sokołowska J, Czajkowski W, Podsiadły R. The photostability of some fluorescent disperse dyes derivatives of coumarin. Dyes Pigm. 2001;49:187–91.
23. Reisfeld R, Zusman R, Cohen Y, Eyal M. The spectroscopic behaviour of Rhodamine 6G in polar and non-polar solvents and in thin glass and PMMA films. Chem Phys Lett. 1988;147:142–7.

Reiß *et al. Heritage Science*   (2023) 11:146

Page 17 of 17

24. Hinde E, Nel P, Sloggett R, Roberts A. Fluorimetric analysis of the constituent dyes within daylight fluorescent pigments: implications for display and preservation of daylight fluorescent artwork. J Am Inst Conserv. 2013;52:97–106.

25. Hyche K, inventor; Company EK, assignee. Fluorescent pigment concentrates. USA Patent WO93/10192. 1993 May 27.

26. Webster JR, inventor; Clariant Finance (BVI) Limited, assignee. Fluorescent pigment compositions. USA Patent 6,683,124 B2. 2004 January 27.

27. Harris R, Becker E, Cabral De Menezes S, Goodfellow R, Granger P. NMR nomenclature. Nuclear spin properties and conventions for chemical shifts. Pure Appl Chem. 2001;73:1795–818.

28. Ferreira BRV, Correa DN, Eberlin MN, Vendramini PH. Fragmentation reactions of Rhodamine B and 6G as revealed by high accuracy orbitrap tandem mass spectrometry. J Braz Chem Soc. 2017;28:136–42.

29. Beltran VL, Druzik J, Maekawa S. Large-scale assessment of light-induced color change in air and anoxic environments. Stud Conserv. 2012;57:42–57.

30. Schmidtke Sobeck SJ, Smith GD. Shedding light on daylight fluorescent artists' pigments, part 2: spectral properties and light stability. J Am Inst Conserv. 2022. https://doi.org/10.1080/01971360.2022.2031460.

Publisher's Note